

A Low-Voltage Rotary Actuator Fabricated Using a Five-Level Polysilicon Surface Micromachining Technology

Thomas W. Krygowski, M. Steven Rodgers, Jeffry, J. Sniegowski, Samuel M. Miller, Jerome Jakubezak

Intelligent Micromachine Department, Sandia National Laboratories,
Albuquerque, New Mexico 87185-1080

Abstract

The design, fabrication and characterization of a low-voltage rotary stepper motor are presented in this work. Using a five-level polysilicon MEMS technology, steps were taken to increase the capacitance over previous stepper motor designs to generate high torque at low voltages. A low-friction hub was developed to minimize frictional loads due to rubbing surfaces, producing an estimated resistive torque of about 6 pN-m. This design also allowed investigations into the potential benefit of using hard materials such as silicon nitride for lining of both the stationary and rotating hub components. The result is an electrostatic stepper motor capable of operation at less than six volts.

I. Introduction

Most electrostatic-actuated micromachined devices utilize fringing fields to produce extended motion. The net force generated is often quite low and requires the application of high operating voltages to overcome dynamic and static friction. Due to the propensity of rubbing surfaces in electrostatic micro-actuators the typical operating voltages are in the tens to hundreds of volts. As a result, electrostatic micro-actuators are not widely used in commercial products. A major effort is underway in the MEMS community to develop a class of actuators that can run at low operating voltages. In this work we present a low-voltage rotary stepper motor, capable of operation in the sub ten-volt range. This order of magnitude reduction in operating voltage was achieved using an electrode configuration designed for self-levitation and a novel hub designed for low-friction operation. To realize this design and achieve this level of performance, Sandia's five-level surface micromachining technology¹ (SUMMiT-V) was employed. This paper is a report on the design, fabrication and initial characterization results for this actuator. Section II reviews an earlier rotary actuator design to illustrate improvements made using a multilevel polysilicon MEMS technology. Section III reviews the SUMMiT-V micromachine technology used in this work, and Section IV presents the device design and characterization results for this low-voltage rotary stepper

motor. This actuator is ideal for a wide range of MEMS applications requiring low-voltage operation, including optical switches, timers and gyros.

II. Device Development

The rotary actuator presented in this work is similar in concept to the variable capacitance side-drive stepper motors first demonstrated in the late 1980's^{2,3}. A side drive stepper motor, shown schematically in figure 1, consists of a set of stationary electrodes (stators) patterned around the perimeter of a conductive polysilicon rotor. During operation a signal pulse is sent to a set of four stator electrodes which align the rotor. The torque generated during this sequence is given by the expression:

$$\tau(\theta) = \frac{1}{2} V^2 \frac{\partial C(\theta)}{\partial \theta} \quad (1)$$

where $\tau(\theta)$ is the torque, V the voltage applied to the stators and $C(\theta)$ the capacitance between the rotor and stator electrodes as a function of angular position. This capacitance is equal to

$$C(\theta) = n \frac{2t\theta\epsilon_0}{\ln \frac{r_2}{r_1}} \quad (2)$$

where n is the number of overlapping electrodes, equal to four in figure 1, t is the (polysilicon) rotor and stator thickness while r_1 and r_2 are the radii of the rotor and stator electrodes respectively. From equation (2) it is clear that the capacitance for this design is small since it is directly proportional to the polysilicon thickness (t), which is only 1-2 μm , and the number of overlapping rotor and stator electrodes are small ($n=4$). The only means to generate higher values of torque with this design is to operate at higher voltages.

In addition to a low capacitance electrode configuration, a second reason for a high operating voltage is the large component of friction in the hub. The rotor shown in figure 1 is constrained to rotate on a hub that

DISCLAIMER

This report was prepared as an account of work sponsored by an agency of the United States Government. Neither the United States Government nor any agency thereof, nor any of their employees, make any warranty, express or implied, or assumes any legal liability or responsibility for the accuracy, completeness, or usefulness of any information, apparatus, product, or process disclosed, or represents that its use would not infringe privately owned rights. Reference herein to any specific commercial product, process, or service by trade name, trademark, manufacturer, or otherwise does not necessarily constitute or imply its endorsement, recommendation, or favoring by the United States Government or any agency thereof. The views and opinions of authors expressed herein do not necessarily state or reflect those of the United States Government or any agency thereof.

DISCLAIMER

Portions of this document may be illegible in electronic image products. Images are produced from the best available original document.

typically has a significant amount of lateral play. This is a byproduct of a fabrication process that introduces a gap between the rotor and hub to allow the rotor to rotate freely after the sacrificial oxides are removed. Unfortunately this also enables the rotor to move freely in the lateral direction. Ideally the electrostatic forces should balance, keeping the rotor centered in the hub. But with sufficient lateral play the rotor can be strongly pulled toward one of the stator electrodes. This effectively slams the rotor into the hub providing a strong normal force and a resulting frictional load in the hub region. This introduces a sliding frictional load due to polysilicon rubbing surfaces in the hub, which must be overcome by high operating voltages to produce rotation.

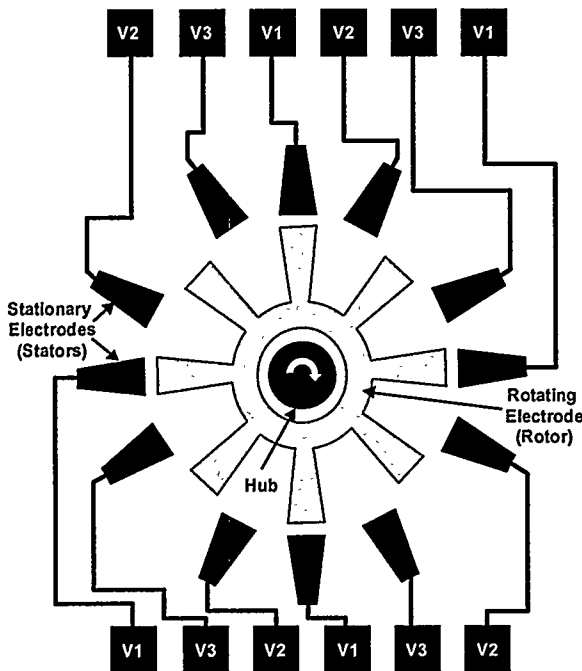


Figure 1. Principle of operation of early side-drive electrostatic micromotors.

The result of a low capacitance electrode configuration and a high-friction hub design, such as in figure 1, is that the drive voltages required are extremely high, in the range of 100-400 volts for early micromotors². This voltage far exceeds what conventional CMOS control circuits can provide, which severely limits their use in mainstream applications. In the present work we have re-examined the side-drive stepper motor and introduced substantial modifications to take advantage of recent advances made in surface micromachining technology. As explained below, surface micromachining has advanced to the point where several layers of mechanical polysilicon can be used to fabricate a more ideal electrode configuration as well as fabricate low-play, low-friction hubs.

III. Technology Overview

Fabrication of the low-voltage rotary stepper motor was accomplished using the five level Sandia Ultra-planar Multi-level MEMS Technology (SUMMiT-V). Figure 2 shows the layer stack of the sacrificial and structural films in the baseline SUMMiT-V technology. The thermal oxide / low-stress silicon nitride stack on top of the substrate electrically isolates the microstructures from the (conductive) substrate. The 0.3 μm poly 0 layer on top of the silicon nitride is typically used for electrical interconnects. The thickness of sacox 1, poly 1, sacox 2 and poly 2 were designed to enable rotating actuators such as the Sandia-developed microengine⁴, as well as the linear actuators, gear trains and hinges required for complex, interactive microsystems. A distinguishing characteristic of the SUMMiT-V technology is the incorporation of Chem-Mechanical Polishing (CMP). CMP is used to planarize sacox 3 and sacox 4 layers to 2 μm thick. By planarizing the sacox 3 and sacox 4 oxide films, the conformal poly 3 and poly 4 films do not reproduce any of the underlying topography. The result is free mechanical movement of the top-most poly films without interference from the underlying patterned films. As explained below, this feature dramatically increases the number of electrodes that are coupled to the rotor as demonstrated below.

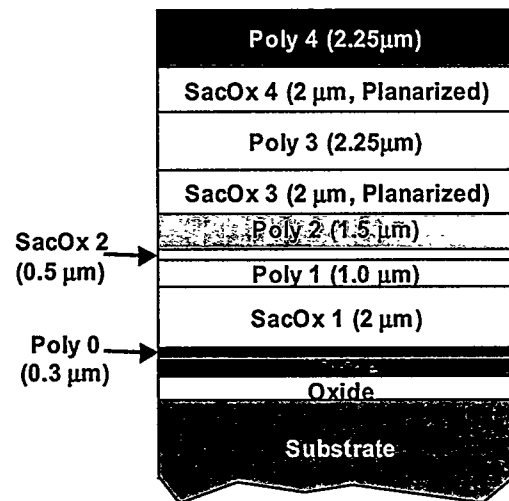


Figure 2. Layer stack for the SUMMiT-V technology, illustrating the five polysilicon films available in the process.

After fabrication is complete, the sacrificial oxides are removed using a 90 minute etch in 1:1 HF:HCl followed by the application of an organic anti-stiction film. This anti-stiction coating generates a hydrophobic surface on polysilicon that prevents the freestanding structures from sticking to the substrate surface during drying.

Modifications to the SUMMIT-V process were made in this work to optimize performance of the low-voltage rotary actuator. As explained below, steps were taken from a technology standpoint to minimize instability of the rotary actuator and to reduce the various components of friction, which together enabled low-voltage operation.

IV. Device Design and Characterization

Figure 3 shows a top view SEM image of the low voltage rotary actuator. To achieve a high torque at low voltages steps were taken to increase the capacitance between the rotor and stator electrodes. Figure 4 shows an SEM image of the electrode structure used in this design. To increase the electrostatic torque, two rotor electrodes couple to each stator element, as opposed to a single rotor/stator pair found in earlier designs (figure 1). Each stator bank consists of three stator electrodes that fan out in the radial direction, and couple to a group of four rotor electrodes. Both the rotor and stator electrodes are fabricated in the same polysilicon level (poly 3) to eliminate out of plane electrostatic coupling. A rotor superstructure is fabricated in the top level of poly (poly 4) to connect the individual rotor elements. By using several concentric rings of rotors and stators the capacitance is dramatically increased allowing for greater torque at lower voltages.

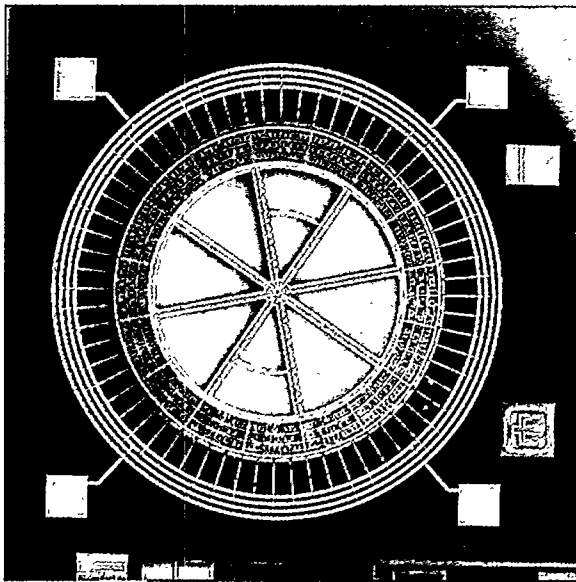


Figure 3. SEM image of low-voltage rotary actuator showing multiple banks of electrodes around the perimeter of the actuator.

To reduce the number of electrical interconnects, the 64 stator banks are arranged in 16 groups of 4 each around the perimeter of the rotor. The first set of stators in each group are connected in parallel by running poly 0 interconnects underneath the rotor, as are the second, third and fourth stator banks in each group. Thus there are only 4 interconnects to the device. The electrical signals are pulse trains with the phasing scheme shown below in figure 5. This study was conducted with the rise of the next pulse being coincident with the fall of the current pulse, although other schemes could be employed.

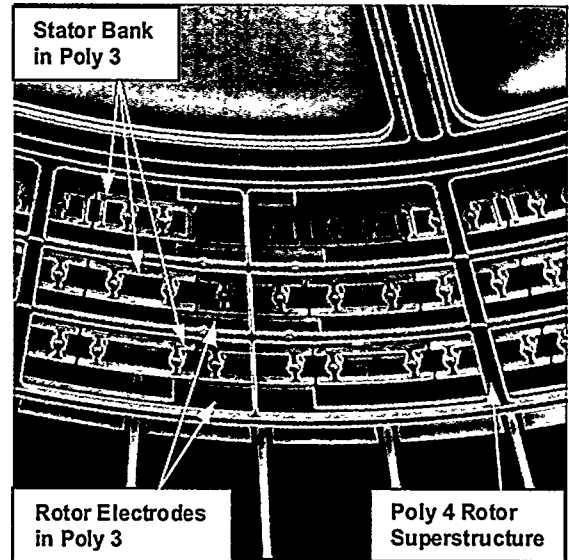


Figure 4. SEM image of low-voltage electrostatic rotary actuator, showing electrode configuration in Poly 3 and rotor in Poly 4.

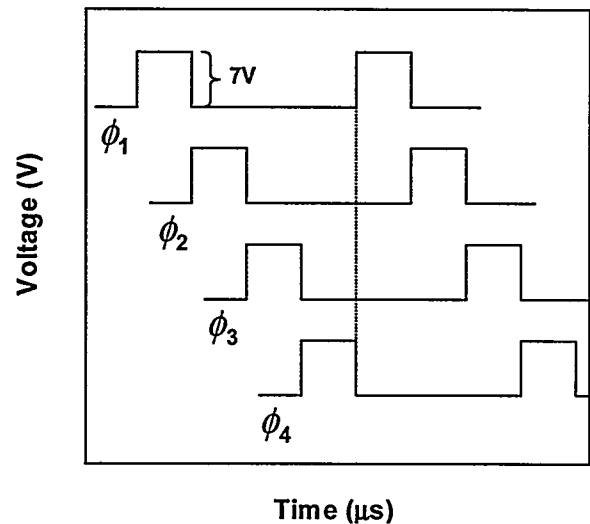


Figure 5. Phasing scheme of signals sent to rotary stepper motor.

An important consequence of the electrode design shown in figure 4 is that the stator fringing fields will levitate and stabilize the rotor. This is shown schematically in Figure 5, where an electric field energy density minimum constrains the rotor to remain in the plane of the stator electrodes. As explained below, this rotor-levitation aspect significantly reduces the contact area of rubbing surfaces in the hub, thus reducing the resistive torque.

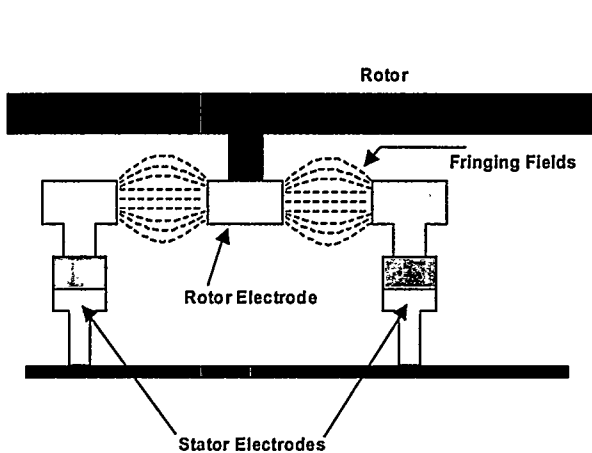


Figure 6. Fringing fields between lateral electrodes levitate the rotor, keeping the rotor electrodes in the same plane as the stator electrodes.

The remaining major source of friction in this device is due to in-plane contact between the rotor pin and the hub. A low-friction hub, shown in figure 7, was designed to minimize the contact area and explore the use of a silicon nitride (SiN) hub lining as a method to reduce friction². Since the fringing fields keep the rotor electrodes vertically centered with the stators, the only rubbing surfaces that remain are between the rotor pin and the hub due to radial motion of the rotor. To reduce the radial travel distance, a thin 0.3- μm sacox 2 layer was used in place of the typical 0.5 μm sacox 2. In addition, a silicon nitride film was deposited in conjunction with sacox 2 that will remain after the release etch.

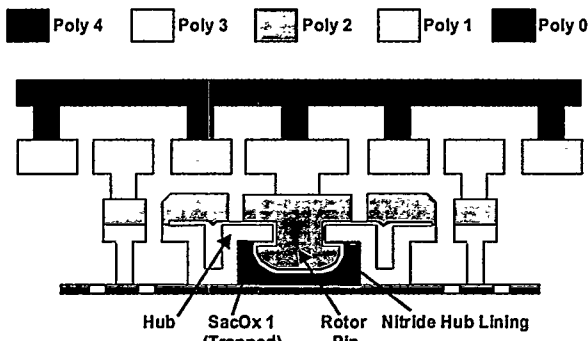


Figure 7. Cross section of actuator, illustrating the low-friction hub design.

Three alternative film stacks were investigated for sacox 2: Case A has SiN-SiO₂-SiN stack, case B a SiN-SiO₂ stack and case C has just the 0.3 μm SiO₂ layer for sacox 2. After removing sacox 2 during the release process, case A will have two contacting surfaces coated with silicon nitride, case B will have nitride and polysilicon in contact and case C will have polysilicon to polysilicon rubbing surfaces in the hub. Table 1 below shows the minimum operating voltage obtained for each case using the phasing scheme outlined in figure 5.

Case	A (SiN-SiO ₂ -SiN)	B (SiN-SiO ₂)	C (SiO ₂)
Min. Voltage	5.7 Volts	5.9 Volts	5.1 Volts

Table 1. Minimum starting voltage for low-voltage stepper motor for cases with and without hub linings.

By implementing these friction reducing designs, we were able to demonstrate fully functioning devices at levels less than six volts in all cases. To allow easy visual verification of proper operation, all testing was performed at low speed with the width of each drive pulse equal to 8.67 ms. At six volts we estimate a very low resistive torque of about $6 \cdot 10^{-12}$ Nm. Thus by employing a new low contact area hub in conjunction with a semi-levitated rotor, we have successfully reduced the major components of friction to a level where low-voltage actuation is now feasible. We believe these results will have a major impact on the implementation of MEMS actuators in CMOS-controlled microsystems.

Acknowledgements

Sandia is a multiprogram laboratory operated by Sandia Corporation, a Lockheed Martin Company, for the United States Department of Energy under Contract DE-AC04-94AL85000.

References

- ¹ J. Sniegowski, S.R. Rodgers, J.H. Smith, *Solid-State Sensor and Actuator Workshop*, Hilton Head Island, SC, June 8-11, 1998.
- ² L.S. Fan, Y.C. Tai, R.S. Mueller, *1988 IEDM Proceedings*, pp. 666.
- ³ M. Mehregany, S. F. Bart, L. S. Tavrow, J. H. Lang, S. D. Senturia, M. F. Schlecht, *Transducers 89'*, pp. 173.
- ⁴ E. J. Garcia and J. J. Sniegowski, *Sensors and Actuators A*, Vol 48, pp. 203-214 (1995).